ISSN 1070-3632, Russian Journal of General Chemistry, 2006, Vol. 76, No. 6, pp. 906–914. © Pleiades Publishing, Inc., 2006.
Original Russian Text © R.M. Aminova, G.A. Shamov, L.I. Savostina, V.F. Mironov, 2006, published in Zhurnal Obshchei Khimii, 2006, Vol. 76, No. 6, pp. 946–955.

Mechanism of the Reaction of 2-Methoxybenzo[*d*][1,3,2]dioxaphosphinin-4-one with Chloral by Quantum-Chemical Calculations

R. M. Aminova[a], G. A. Shamov[a], L. I. Savostina[a], and V. F. Mironov[b]

[a] *Kazan State University, ul. Kremlevskaya 18, Kazan, Tatarstan, 420008 Russia*
[b] *Arbuzov Institute of Organic and Physical Chemistry, Kazan Research Center, Russian Academy of Sciences, Kazan, Tatarstan, Russia*

Received May 11, 2005

Abstract — Quantum-chemical calculations of various stereoisomers, intermediates, and transition states of the reaction of 2-methoxybenzo[*d*][1,3,2]dioxaphosphinin-4-one with chloral, leading to formation of 2-methoxy-3-(trichloromethyl)benzo[*e*][1,4,2λ^5]dioxaphosphepin-2,5-dione, were carried out by the density functional theory (DFT) method with the PBE functional and Triple *z* basis, using the Priroda program. The first step of the reaction is [1 + 2] cycloaddition of phosphorus to the chloral C=O bond to form an intermediate with a five-coordinate phosphorus atom via a transition state in which the positive and negative charges are strongly localized on phosphorus and chloral oxygen, respectively. Calculations of the internal reaction coordinate from all transition states were carried out.
DOI: 10.1134/S1070363206060107

Cyclic phosphorous derivatives of salicylic acid (2-RO-benzo[*d*][1,3,2]dioxaphosphinin-4-ones or salicyl phosphites) containing a chiral phosphorus atom are convenient objects for mechanistic research on reactions with carbonyl compounds, since using prochiral aldehydes and ketones can result in diastereomer formation and thus provide additional evidence to explain why one or another reaction pathway is realized.

Reactions of salicyl phosphites with halocarbonyl derivatives (e.g. bromal, chloral, and fluoral) are of special interest, because they can take different pathways and lead to formation of compounds with a phosphorus–carbon bond under very mild conditions. Among products obtained from chloral, highly active insecticides [1] and effective remedies for Alzheymer disease [2] have been found.

Previously we found that one of the pathways of the reaction of salicyl phosphites with carbonyl compounds activated by electron-acceptor substituents (such as chloral, trifluoroacetone, ethyl piruvate, and hexafluoroacetone) involves extension of the initial six-membered ring to seven-membered to form 2-RO-benzo[*e*][1,3,2]dioxaphosphepin-5-ones or 2-RO-benzo[*e*][1,4,2]dioxaphosphepin-5-ones. Basing on abundant experimental evidence we showed that these reactions feature a high degree of stereoselectivity [3–9], i.e. one of the two possible diastereomers is formed in preference to the other (>95%). It was suggested that the first step of these reactions involves the rate-limiting bimolecular reaction of a nucleophilic center, the phosphorus atom of phosphite **I**, with the C=O carbon atom as the electrophilic center (this was confirmed by kinetic experiments [10–14]). The subsequent intramolecular nucleophilic attack of the alkoxide anion in dipolar ion **A** formed on the endocyclic carbon atom of the carbonyl group leads to final reaction product **II**. The formation of the intermediate zwitterion or betaine **A** is usually postulated. Therewith, it is also suggested that, depending on the nature of the exocyclic substituent on phosphorus, dipolar ion **A** can also undergo a variety of other transformations. One of them is formation of a P^+–O–C^-dipolar ion (when the starting carbonyl compound contains fragments capable of stabilizing the negative charge on carbon, such betaines are quite stable [10]).

It terms of the ionic mechanism thoroughly substantiated by a great body of experimental data [10, 11], the reaction with chloral leading to phosphepines **II** can be schematically presented by the following elementary transformation sequence (Scheme 1).

Mironov et al. [16] have thoroughly described the synthetic material, as well as the X-ray diffraction analysis of the reaction products. The reasons for the high stereoselectivity of the reaction are rather difficult to reveal, in particular, because of the lack of inform-

Scheme 1.

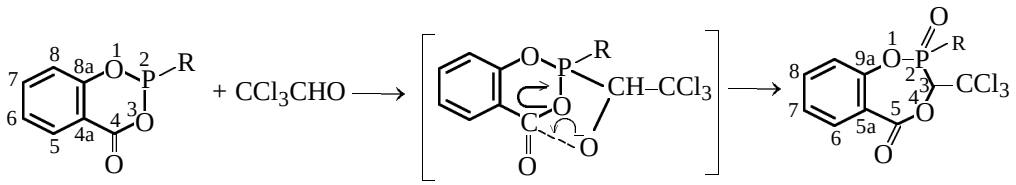

Ia–If **A** **IIa–IIf**

R = OCH_3 (**a**), $OCH_2CH_2CH_2CH_3$ (**b**), OCH_2CF_3 (**c**), $OCH_2CF_2CHF_2$ (**d**), OC_6F_5 (**e**), Ph (**f**).

ative experimental data on the reaction kinetics in the gas phase and in media of various polarity.

It is evident from the aforesaid that elucidation of the mechanism and explanation of the stereochemical result of such reactions is an important theoretical problem which can be solved by means of modern methods of quantum chemistry.

Previously [17] we studied the structure of all possible diastereomeric products of the reaction of salicyl phosphites with chloral by means of semiempirical MNDO, AM1 and PM3 methods. Some preliminary results concerning the structures of suggested intermediates considered in the present work were reported in [18–25].

The aim of the present work was to study the reaction of 2-methoxybenzo[*d*][1,3,2]dioxaphosphinin-4-one (**Ia**) with chloral (Scheme 1), leading to 1,4,2-dioxaphosphepine **IIa** under mild conditions, by means of modern quantum-chemical methods. We recently performed quantum-chemical calculations of the transition states, reagents, and reaction products by the DFT method with the PBE functional and Triple *z* basis using the Priroda program [26].

The calculations showed that the molecule of salicyl phosphite **Ia** in the ground state has the heterocyclic fragment in a flattened distorted *boat* conformation ($P^2O^1C^{8a}C^{4a}$ and $P^2O^3C^4C^{6a}$ dihedral angles are –24.1° and 7.1°, respectively) with a planar $O^1C^{8a}\cdot C^{4a}C^4$ fragment and the P^2 and O^3 atoms deviating from this plane to the same side but by different distances, or a *sofa* conformation with a planar five-atomic $O^1P^2O^3C^4C^{4a}C^{8a}$ fragment with the phosphorus atom only slightly deviating from this plane. Figures 1a and 1b show a general view of the molecule in two projections. Selected geometric parameters (interatomic distances and bond and torsion angles) are listed in Table 1. The carbonyl group insignificantly deviates from a planar $O^1C^{8a}C^{4a}C^4$ fragment ($O^4C^4C^{4a}C^{8a}$ dihedral angle –172.3°). The OCH_3 substituent occupies the axial position owing to the anomeric effect [27], and its methyl group points away from the benzo fragment.

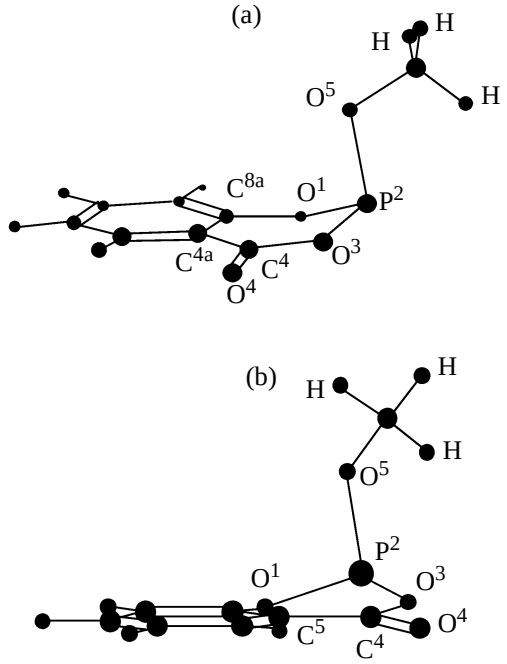

Fig. 1. Spatial arrangement of the molecule of phosphite **Ia** as viewed from the (a) carbonyl group and (b) benzo fragment.

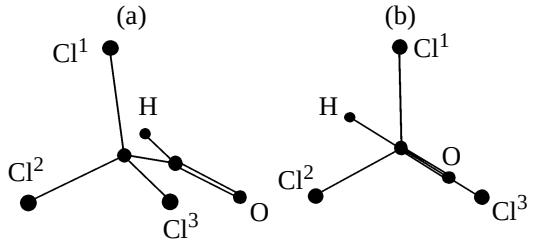

Fig. 2. Spatial arrangement of the chloral molecule as viewed from the (a) trichloromethyl and (b) carbonyl groups.

The molecular geometry of chloral was also optimized. With respect to the C–C bond, the molecule has a conformation in which one of the chlorine atoms is eclipsing the C=O bond (the $Cl^3C^2C^1O$ and $Cl^3C^2C^1H$ dihedral angles are 0° and 180°, respectively). Figures 2a and 2b show a general view of the

Table 1. Selected interatomic distances (Å) and bond and torsion angles (deg) in phosphite **Ia**

Bond	*d*	Angle	ω	Angle	τ
P^2–O^1	1.721	$P^2O^1C^{8a}$	122.5	$P^2O^1C^6C^5$	–24.1
P^2–O^3	1.710	$P^2O^3C^4$	125.7	$P^2O^3C^4C^5$	7.1
C^{4a}–C^{8a}	1.410	$O^3C^4C^{4a}$	120.3	$P^2O^3C^4O^7$	–174.6
C^4–C^{4a}	1.483	$O^3P^2O^1$	100.5	$O^1C^6C^5C^4$	3.4
C^{8a}–O^1	1.355	$C^4C^{4a}C^{8a}$	121.4	$O^1P^2O^3C^4$	–21.7
C^4–O^4	1.214	$O^3C^4O^4$	111.5	$C^6O^1P^2O^3$	29.8
C^4–O^3	1.351	$O^4C^4C^{4a}$	128.2	$C^6C^5C^4O^3$	5.6
		$C^{4a}C^{8a}O^1$	22.7	$C^6C^5C^4O^7$	–172.3

Table 2. Selected intratomic distances (Å) and bond and torsion angles in chloral

Bond	*d*	Angle	ω	Angle	τ
C^1–C^2	1.553	OC^1H	124.4	$OC^1C^2Cl^1$	121.7
C^1–O	1.202	OC^1C^2	124.2	$OC^1C^2Cl^2$	–121.8
C^1–H	1.113	HC^1C^2	111.4	$OC^1C^2Cl^3$	0
C^2–Cl^1	1.804	$Cl^1C^2C^1$	105.7	$HC^1C^2Cl^1$	–58.3
C^2–Cl^2	1.804	$Cl^2C^2C^1$	105.7	$HC^1C^2Cl^2$	58.3
C^2–Cl^3	1.776	$Cl^3C^2C^1$	112.8	$HC^1C^2Cl^3$	180.0

chloral molecule in two projections, and Table 2 lists its geometric parameters. Calculations with geometry optimization, starting from the initial geometry with chlorine and oxygen *trans* to each other, too, gave an eclipsed conformation with an energy of –1531.983601 au (corrected for zero-point energy).

The electronic and steric structure of 1,4,2-dioxaphosphepines **IIa** and **IIf** formed by the reaction of salicyl phosphites **Ia** and **If** with chloral we studied previously by semiempirical quantum-chemical methods [17] to show that the preferred conformations are distorted *chair* and distorted *boat* (Fig. 3). The results of our DFT calculations by the program [26] for these heteroring conformations in diastereomers with different substituent orientations are presented in Table 3 and Fig. 3 together with PM3 results. Table 4 lists selected geometric parameters for calculated structures **1**–**8** of diastereomers of compound **IIa**.

The calculations gave two intermediates **III** and **IV** with a five-coordinate phosphorus. Their geometry is shown in Figs. 4 and 5, and their principal geometric parameters are listed in Table 5. Evidently, the first reaction act involves a symmetry-allowed chele-

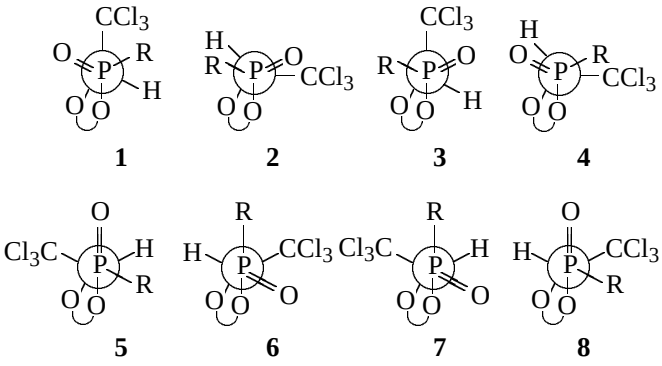

tropic process, i.e. [1+2] cycloaddition of phosphorus having a lone electron pair and vacant *d* orbitals, by the C=O bond. The CCl_3 and OCH_3 groups in intermediate **III** are *cis* to each other, that is they locate on the same side of the three-membered $P^2O^7C^8$ heteroring. The total energy of this intermediate is 2482.607621 au. The six-membered heteroring has a *sofa* conformation with a planar pentaatomic $O^1C^6 \cdot C^5C^4O^2$ fragment and the phosphorus atom noticeably deviating from it. The methoxy group locates in the axial position of this heteroring, and the C^8 and O^7

Table 3. Total energies E^t (corrected for zero-point energy) of enantiomers of benzo[*e*][1,4,2]dioxaphosphepine **IIa**, calculated by the DFT method, in comparison with the results of PM3 semiempirical calculations

Comp. no.	Configuration of izomer and conformation of heteroring	E^{tot}, au (DFT)	E^{tot}, au (PM3)	ΔH, kcal nol^{-1} (PM3)
1	S_PR_C, *bauch*	–2482.633695	–3848.5581	–213.9554
2	R_PS_C, *bauch*	–2482.629124	–3848.4143	–210.6298
3	R_PR_C, *bauch*	–2482.634038	–3848.5001	–212.6142
4	S_PS_C, *bauch*	–2482.627172	–3848.4546	–211.5676
5	S_PR_C, *chair*	–2482.621545	–3848.2459	–206.7543
6	R_PS_C, *chair*	–2482.624216	–3848.3412	–208.9539
7	R_PR_C, *chair*	–2482.620627	–3848.26292	–207.1467
8	S_PS_C, *chair*	–2482.622456	–3848.3082	–208.1906

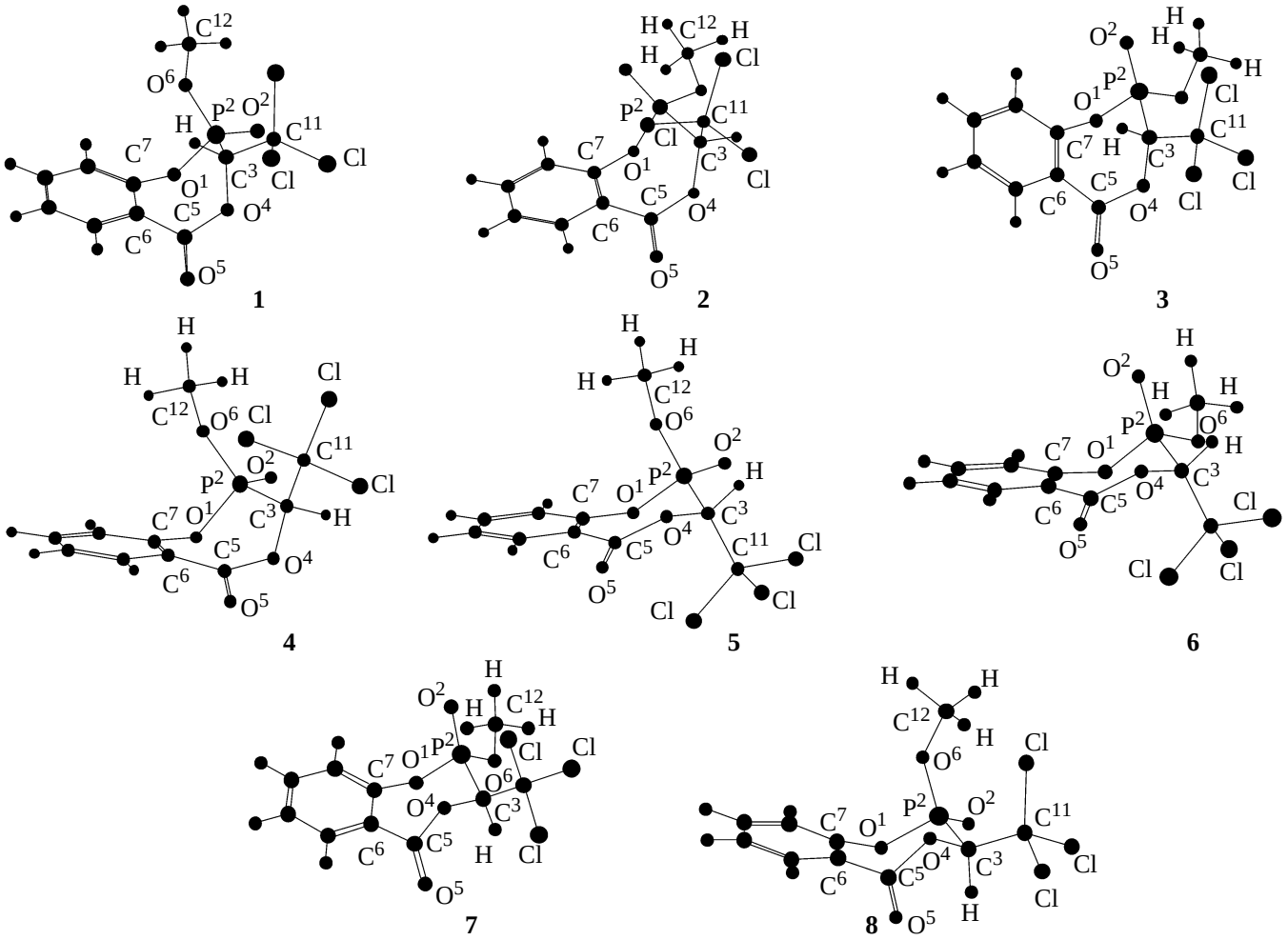

Fig. 3. Spatial arrangement of the calculated conformations of enantiomers of 2-methoxy-3-(trichloromethyl)benzo[*e*]-[1,4,2λ^5]dioxaphosphepine-2,5-dione (**IIa**).

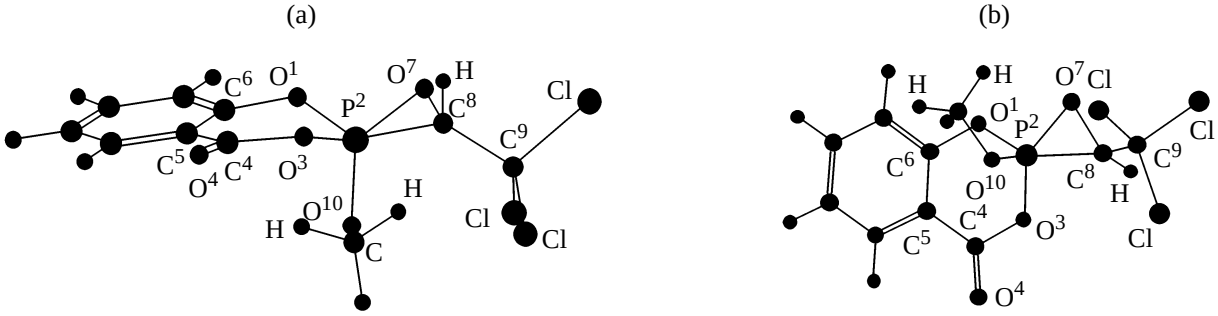

Fig. 4. Structure of five-coordinate intermediate **III** with the energy –2482.607621 au, as viewed from the (a) C^4=O^4 carbonyl group and (b) P^2–O^{10} bond.

atoms are equatorial. That means that the resulting three-membered $P^2O^7C^8$ ring plane is in the equatorial position. The tree-membered ring has *trans* orientation with the respect to the C^4=O^4 bond. In spirophosphorane **III**, the configuration of the phosphorus atom is more likely distorted square pyramid than trigonal bipyramid. Hence, the $O^3P^2O^7$ bond angle between the substituents that, by the apicophilicity rule, should be axial, is 133.6° in intermediate **III** and 93.1° in intermediate **IV**. Only a few fove- and six-coordinate phosphorus compounds with three-membered rings have been described [28, 29]. The most close to intermediate **III** or **IV** is structure **V** with a selenaphosphirane ring, 3,3'-dimethyl-1-phenyl-3,3-bis(tri-

Table 4. Selected interatomic distances (Å) and bond (ω) and torsion (τ) angles in stereoisomers of phosphepine **IIa**

Parameter	**1**	**2**	**3**	**4**	**5**	**6**	**7**	**8**
Bond				*d*				
P^2–O^1	1.654	1.655	1.655	1.650	1.641	1.645	1.664	1.652
P^2–C^3	1.887	1.892	1.891	1.891	1.871	1.871	1.888	1.890
P^2–O^2	1.487	1.491	1.492	1.489	1.488	1.492	1.490	1.488
P^2–O^6	1.623	1.618	1.607	1.617	1.623	1.608	1.614	1.617
O^1–C^7	1.394	1.397	1.397	1.394	1.388	1.390	1.395	1.393
C^6–C^7	1.406	1.405	1.406	1.405	1.409	1.407	1.408	1.408
C^5–C^6	1.493	1.494	1.493	1.494	1.506	1.502	1.485	1.484
C^5–O^4	1.390	1.402	1.392	1.400	1.403	1.410	1.416	1.416
O^4–C^3	1.428	1.420	1.427	1.420	1.420	1.424	1.427	1.425
C^5–O^8	1.208	1.209	1.208	1.209	1.209	1.208	1.203	1.203
C^3–C^{11}	1.544	1.548	1.544	1.550	1.554	1.555	1.539	1.540
O^6–C^{12}	1.456	1.457	1.457	1.456	1.457	1.458	1.456	1.457
Bond angle				ω				
$O^1P^2C^3$	99.3	100.6	98.3	101.3	104.7	104.2	99.0	97.9
$O^1P^2O^9$	111.3	114.4	115.0	111.3	110.7	115.4	114.9	111.1
$O^1P^2O^6$	104.3	100.6	99.9	104.7	106.0	100.5	98.7	102.4
$P^2C^3O^4$	110.1	115.4	112.0	116.0	112.9	108.1	101.6	103.8
$P^2C^3C^{11}$	115.6	115.1	117.3	117.7	117.6	122.1	118.1	119.0
$P^2O^1C^7$	119.8	114.2	116.7	–70.0	124.8	121.4	127.3	129.6
$O^2P^2O^6$	117.8	118.1	118.5	118.0	117.2	118.0	118.6	118.1
$O^6P^2C^3$	100.6	98.7	106.8	106.8	97.0	106.1	102.9	106.1
$O^2P^2C^3$	121.0	121.0	115.5	113.1	119.5	111.1	119.2	118.3
$C^3O^4C^5$	120.7	127.5	121.0	127.1	129.5	129.6	117.2	117.4
$C^{11}C^3O^4$	106.9	112.9	107.0	112.5	111.7	111.7	109.3	110.0
$O^4C^5O^5$	118.0	116.1	117.9	116.3	115.1	115.6	122.9	122.3
$O^5C^5C^6$	123.6	122.1	123.8	122.1	120.9	121.4	128.5	127.2
$O^4C^5C^6$	118.4	121.4	118.3	121.3	123.1	122.0	108.6	110.5
$C^5C^6C^7$	122.9	125.5	122.6	125.7	129.9	128.6	117.1	119.8
$O^1C^7C^6$	120.7	121.1	119.8	122.1	125.2	123.5	119.6	121.3
$C^{12}O^6P^2$	118.7	117.7	119.3	119.2	117.7	118.0	118.2	119.3
Torsion angle				τ				
$O^1P^2C^3O^4$	41.3	–6.5	35.1	0.3	–62.0	–65.4	–53.2	–56.5
$O^1P^2C^3C^{11}$	162.5	–140.7	159.4	–137.2	70.4	66.3	–172.7	–179.1
$O^1P^2O^6C^{12}$	–107.4	89.4	113.7	–108.0	–89.2	92.1	94.3	–135.3
$P^2C^3O^4C^5$	–86.2	–60.8	–83.4	–64.8	61.6	66.1	90.7	92.1
$P^2O^1C^7C^6$	–76.6	–72.7	–81.5	–70.0	–50.4	–57.3	–77.5	–71.6
$O^2P^2O^6C^{12}$	16.5	–35.8	–12.0	15.5	34.9	–34.2	–30.4	–12.9
$O^6P^2C^3O^4$	147.8	–109.2	–67.9	109.6	46.6	–171.0	–154.3	48.9
$O^2P^2C^3O^4$	–80.6	120.5	158.0	–119.0	173.4	59.5	72.1	–175.6
$C^3O^4C^5O^5$	–158.1	–142.7	–158.3	–142.5	138.9	131.7	69.9	79.7
$C^3O^4C^5C^6$	23.3	43.8	23.1	44.0	–51.4	–59.6	–110.6	–103.2
$C^{11}C^3O^4C^5$	147.5	74.3	146.8	74.8	–73.6	–71.0	–143.7	–139.6
$O^5C^5C^6C^7$	–137.6	–151.7	–137.5	–152.4	–160.4	–156.6	–125.1	–132.0
$O^4C^5C^6C^7$	41.0	21.4	41.0	20.8	30.6	35.5	55.4	51.0
$C^5C^6C^7O^1$	–0.8	–5.5	–0.3	–5.7	1.7	3.2	10.7	9.2
$C^{12}O^6P^2C^3$	150.1	–168.1	–144.5	144.1	163.3	–159.6	–164.3	122.6

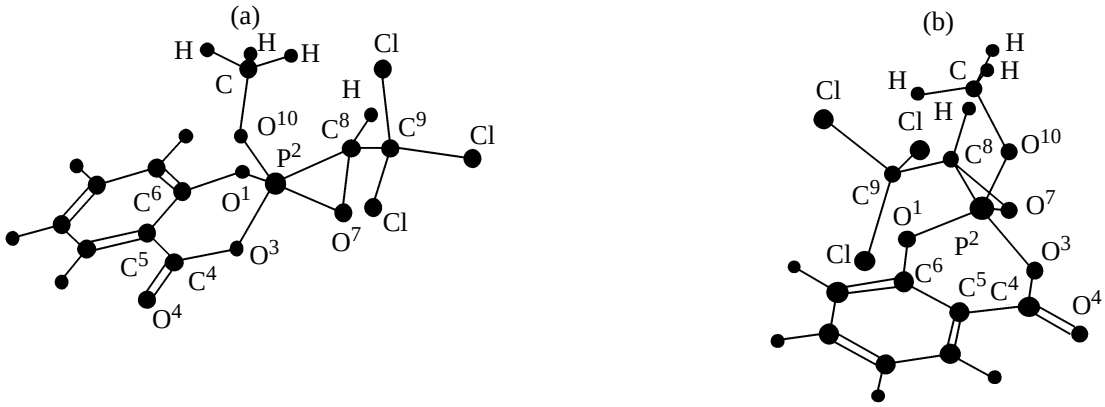

Fig. 5. Structure of five-coordinate intermediate **IV** with the energy –2481.609111 au, as viewed from the (a) $C^4{=}O^4$ carbonyl group and (b) phenylene fragment.

Table 5. Selected interatomic distances (Å) and bond and torsion angles (deg) in prereaction complexes and transition states

Parameter	**III**	**IV**	TS_{III}	TS_{IV}	Parameter	**III**	**IV**	TS_{III}	TS_{IV}
Bond		*d*			Bond		*d*		
$P^2–O^1$	1.700	1.658	1.639	1.647	$O^3–C^4$	1.414	1.390	1.698	1.686
$P^2–O^3$	1.664	1.673	1.568	1.563	$O^4–C^4$	1.206	1.208	1.184	1.184
$P^2–O^7$	1.645	1.633	2.417	2.418	$C^4–C^5$	1.470	1.478	1.483	1.485
$P^2–O^{10}$	1.614	1.627	1.599	1.596	$C^5–C^6$	1.407	1.403	1.405	1.405
$P^2–C^8$	1.803	1.817	1.874	1.865	$O^1–C^6$	1.369	1.386	1.401	1.401
$O^7–C^8$	1.515	1.515	1.343	1.344	$O^{10}–C^{12}$	1.454	1.450	1.467	1.467
$C^8–C^9$	1.507	1.508	1.553	1.565	$O^7–C^4$	2.016	2.025		
Bond angle		ω			Bond angle		ω		
$O^1P^2O^3$	97.6	99.6	105.9	106.0	$O^3P^2C^8$	98.5	144.6	101.2	107.5
$O^1P^2O^7$	90.8	127.6	34.5	34.3	$O^3C^4O^4$	117.5	119.1	39.8	39.3
$O^1P^2C^8$	139.3	100.3	109.2	102.6	$O^4C^4C^5$	126.3	125.3	131.5	130.9
$O^1P^2O^{10}$	101.1	109.1	105.5	104.6	$C^4C^5C^6$	121.6	122.0	122.6	123.0
$P^2O^3C^4$	127.2	126.4	56.9	35.6	$P^2O^{10}C^{12}$	120.4	119.9	120.1	120.1
$P^2C^8O^7$	58.7	70.4	96.0	96.5	$C^5C^6O^1$	122.7	123.3	122.7	122.7
$P^2C^8C^9$	133.5	130.7	117.9	115.7	$C^6O^1P^2$	121.8	123.2	119.3	118.7
$P^2O^7C^8$	58.7	70.4	96.0	96.5	$O^7P^2C^8$	51.9	57.8	33.6	33.5
$O^7C^8C^9$	116.4	114.7	115.8	117.6	$O^3P^2O^7$	133.6	93.1	81.8	81.7
$O^3P^2O^{10}$	105.7	94.4	111.7	112.7	$O^{10}P^2O^7$	117.3	120.4	155.9	155.0
					$O^{10}P^2C^8$	110.0	106.2	122.4	121.9
Torsion angle		τ			Torsion angle		τ		
$C^9C^8P^2O^{10}$	11.5	–147.4	55.7	–48.6	$P^2O^7C^8C^9$	126.7	–123.9	125.0	–123.5
$O^3P^2C^8C^9$	121.8	89.5	–179.4	83.6	$O^3P^2O^{10}C^{12}$	145.2	–170.5	50.3	49.1
$O^1P^2O^3C^4$	34.8	–36.9	33.9	33.8	$O^4C^4C^5C^6$	171.0	–177.0	–177.6	–177.0
$O^1P^2O^7C^8$	–27.9	71.3	–128.9	–113.4	$C^5C^6O^1P^2$	25.7	–12.3	5.9	5.5
$O^1P^2C^8O^7$	162.2	–130.3	55.5	70.1	$C^6O^1P^2O^3$	–38.5	28.0	28.6	29.2
$O^1P^2O^{10}C^{12}$	43.9	–68.7	–64.3	–65.5	$C^6O^1P^2O^{10}$	69.2	–70.1	147.1	148.5
$P^2O^3C^4O^4$	165.3	–157.0	56.9	–143.6	$C^6O^1P^2O^7$	–172.8	129.5	42.4	41.5
$P^2O^3C^4C^5$	–16.0	26.9	41.0	40.5	$C^6O^1P^2C^8$	–151.2	178.6	–79.7	–83.4

fluoromethyl)spiro[2*H*-2,1]benzo-1,2λ^5-oxaphospholo[1,2]selenaphosphirane [29]. In this compound, the POSe bond angle (the oxygen and selenium atoms are in the axial positions) is 155.82(6)°. Our calculated structure of intermediate **III** or **IV** is much more distorted to square pyramid than the structure of phosphorane **V**.

The other calculated intermediate **IV** contains a six-membered heteroring whose conformation, too, is *sofa* with a planar $O^1C^6C^5C^4O^3$ pentaatomic fragment. In this heteroring, the methoxy group occupies the axial position, and the O^7 and C^8 atoms are equatorial. The $P^2O^7C^8$ three-membered heteroring is turned so that its oxygen atom is *cis* to the exocyclic carbonyl bond $C^4{=}O^4$. This oxygen is roughly coplanar with the $P^2{-}O^3$ bond. The CCl_3 substituent in the three-membered ring is *trans* to the OMe group. That is, the CCl_3 and OMe groups locate on different sides of the $P^2O^7C^8$ plane. The energy of intermediate **IV** is –2482.609111 au. Similarly to intermediate **III**, the configuration of the five-coordinate phosphorus atom in phoshorane **IV** is much distorted to square pyramid.

Further calculations gave two transition states TS_{III} and TS_{IV}. They locate on the pathway of transformation of intermediates **III** and **IV** to diastereomeric reaction products **IIa**. The energies and frequencies for these transition states are as follows.

	Total energy without inclusion of zero-point energy	Zero-point energy	Total energy with inclusion of zero-point energy	Frequency, cm^{-1}
TS_{III}	–2482.754273	0.165588	–2482.588685	222.0 (*i*)
TS_{IV}	–2482.755885	0.165509	–2482.590380	219.7 (*i*)

Table 5 lists selected geometric parameters of these transition states.

Figure 6 shows the structure of transition state TS_{III} in three projections. In TS_{III}, the distance from the O^7 atom which practically hangs over the six-membered heteroring to the C^4 atom is 1.82 Å. At the same time, the $C^4{=}O^4$ bond is noticeably shorter (1.184 Å) than in starting intermediate **III** (1.207 Å); the interatomic distance $P^2{-}O^3$ (1.568 Å) is also shorter than in phosphorane **III**. Its length is intermediate between the single P–O and double $P^2{=}O^2$ bond lengths in phosphepine **IIa** (1.487–1.491 Å). In transition state TS_{III}, the $O^3{-}C^4$ bond is elongated (1.698 Å). In phosphorane **III**, it is equal to 1.414 Å. These data suggest that the $O^3{-}C^4$ bond is significantly loosened and that the geometry of the $C^4{-}O^4$ group becomes close to that of the acylium cation. At the same time, the configuration of the phosphorus atom becomes tetrahedral (bond angles at phosphorus are 105.9–111.7°). The $O^7{-}C^8$ bond (1.343 Å) in transition state TS_{III} is much shortened compared to intermediate **III** (1.515 Å). Taking account of the C=O distance in chloral (1.202 Å), we can suggest that the oxygen atom in TS_{III} is essentially anionoid.

Figure 7 depicts the structure of transition state TS_{IV} in two projections. Like with TS_{III}, the O^7 atom in transition state TS_{IV} hangs over C^4, and the distance between them is 2.025 Å. Contrary to that, PM3 calculations [17–21] result is an expressed bicyclic structure, while in the case in hand the $O^3{-}C^4$ bond (1.686 Å) is ruptured.

Both in TS_{III} and in TS_{IV}, all atoms of the seven-membered heteroring and phenylene fragment lie in one plane, except for O^3 that deviates from this plane to the side opposite to O^7. Note also that TS_{III} and TS_{IV} have similar structural and energetic parameters,

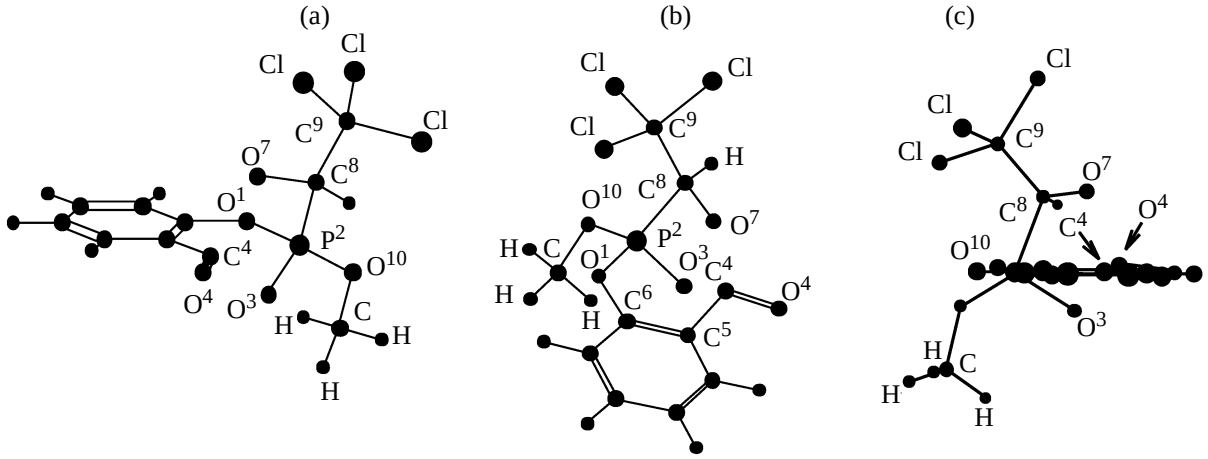

Fig. 6. Structure of transition state TS_{III} as viewed from the (a) carbonyl group, (b) CCl_3 group, and (c) phenylene fragment.

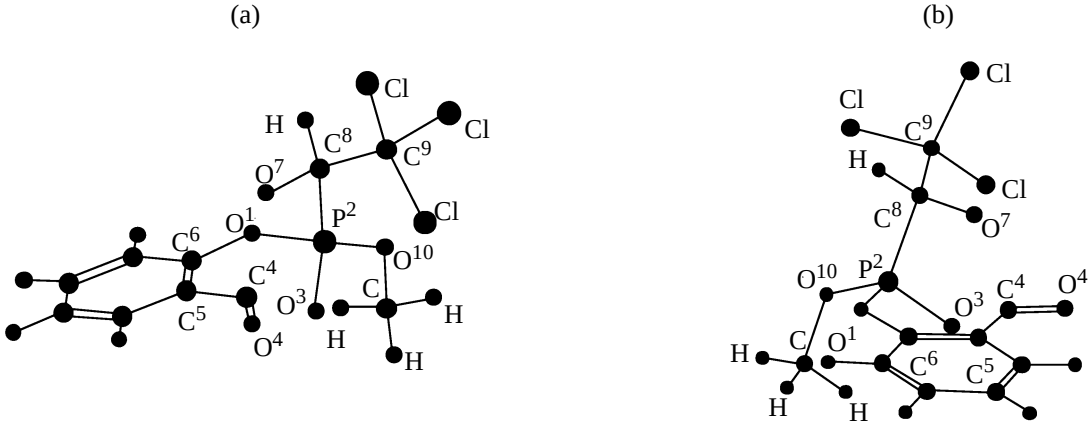

Fig. 7. Structure of transition state TS_{IV} as viewed from the (a) $C^4{=}O^4$ and (b) CCl_3 groups.

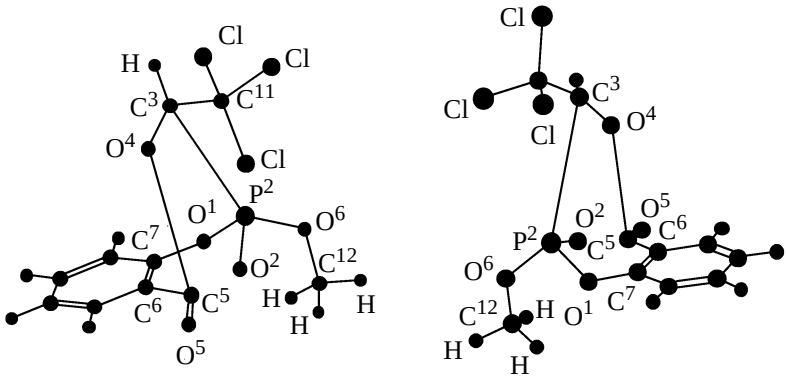

Fig. 8. Structure obtained by calculation of the internal reaction coordinate from the top of transition state TS_{III} to the starting reagents (view in two projections).

which makes the fact that one diastereomer is much preferred over the other impossible to explain.

We calculated the internal reaction coordinate. The resulting data are shown in Fig. 8. It was found that the descent from the top of the potential barrier along one the directions leads to structures in which the chloral molecule is detached from salicyl phosphite **IIa**. The distance between the carbonyl carbon atom and the oxygen atom of the detached chloral molecule is 3.858 Å. Calculation of the internal reaction coordinate along the other direction resulted in formation of a seven-membered heteroring.

We performed quantum-chemical calculations of the energies of transition states TS_{III} and TS_{iV} with inclusion of solvent (chloral) effects within the framework of the polarized continuum model (PCM) by means of the GAMESS program [30]. The calculations resulted in an only slight increase in the energy gap between the transition states (~1.88 kcal mol^{-1}): The energies of transition states TS_{III} and TS_{IV} in the solvent are –2476.61368653 and –2476.61674899 au, respectively. As seen, the inclusion of solvent effects within PCM does not allow to explain the high stereoselectivity of the reaction. Nevertheless, we suggest that solvent effects play an important role in this process. In future calculations with inclusion of solvent effects in the framework of the supermolecular approach are required, focusing on salicyl phosphite–chloral clusters.

ACKNOWLEDGMENTS

The work was financially supported by the Russian Foundation for Basic Research (regional project no. 03-03-96214p2003Tatarstan) and the Research and Experimental Development Foundation of Tatarstan [project no. 06-0.3-154/2002F(06)].

REFERENCES

1. Hudson, H.R., Jaszay, Z.M., and Pianka, M., *Phosphorus, Sulfur, Silicon Relat. Elem.*, 2003, vol. 178, no. 7, p. 1571.

2. Mashkovskii, M.D. and Glushkov, R.G., *Khim-Farm. Zh.*, 2001, vol. 35, no. 4, p. 3.
3. Mironov, V.F., Konovalova, I.V., Mavleev, R.A., Mukhtarov, A.Sh., Ofitserov, E.N., and Pudovik, A.N., *Zh. Obshch. Khim.*, 1991, vol. 61, no. 10, p. 2150.
4. Mironov, V.F., Burnaeva, L.M., Konovalova, I.V., Khlopushina, G.A., Mavleev, R.A., Chernov, P.P., and Pudovik, A.N., *Zh. Obshch. Khim.*, 1993, vol. 63, no. 1, p. 25.
5. Mironov, V.F., Burnaeva, L.A., Krokhalev, V.M., Saloutin, V.I., Konovalova, I.V., Mavleev, R.A., and Chernov, P.P., *Zh. Obshch. Khim.*, 1992, vol. 62, no. 6, p. 1425.
6. Mironov, V.F., Mavleev, R.A., Burnaeva, L.A., Konovalova, I.V., Pudovik, A.N., and Chernov, P.P., *Izv. Akad. Nauk, Ser. Khim.*, 1993, no. 3, p. 565.
7. Mironov, V.F., Konovalova, I.V., Burnaeva, L.M., Khlopushina, G.A., and Shastina, Yu.S., *Zh. Obshch. Khim.*, 1994, vol. 64, no. 7, p. 1217.
8. Mironov, V.F., Burnaeva, L.M., Khlorushina, G.A., Konovalova, I.V., Kurykin, M.A., and Rakhmatullin, A.I., *Izv. Akad. Nauk, Ser. Khim.*, 1996, no. 12, p. 3008.
9. Mironov, V.F., Burnaeva, L.M., Gubaidullin, A.T., Litvinov, I.A., Konovalova, I.V., Zyablikova, T.A., Ivkova, G.A., and Romanov, S.V., *Zh. Obshch. Khim.*, 1998, vol. 68, no. 3, p. 399.
10. Vladimirova, I.L., Grapov, A.F., and Lomakina, V.I., *Reakts. Metody Issled. Org. Soedin.*, 1966, vol. 16.
11. Luknitskii, F., *Chem. Rev.*, 1975, vol. 75, no. 3, p. 259.
12. Borowitz, I.J., Firstenberg, S., Borowitz, G.B., and Schuesler, D., *J. Am. Chem. Soc.*, 1972, vol. 94, no. 5, p. 1623.
13. Borowitz, I.J. and Crouch, R.K., *Phosphorus*, 1973, vol. 2, p. 209.
14. Gaudau, E.M. and Bianchini, J.P., *Can. J. Chem.*, 1976, vol. 54, no. 22, p. 3626.
15. Petnehazy, I., Szakal, G., Toke, L., Hudson, R., Powroznyk, L., and Cooksey, S.J., *Tetrahedron*, 1983, vol. 39, no. 24, p. 4229.
16. Mironov, V.F., Litvinov, I.A., Gubaidullin, A.T., Aminova, R.M., Burnaeva, L.M., Azancheev, N.M., Filatov, M.E., and Konovalova I.V., *Zh. Obshch, Khim.*, 1998, vol. 68, no. 7, p. 1080.
17. Aminova, R.M., Mironov, V.F., and Filatov, M.E., *Zh. Obshch, Khim.*, 1999, vol. 69, no. 1, p. 58.
18. Aminova, R.M., Mironov, V.F., Filatov, M.E., and Savostina, L.I., *Zh. Obshch. Khim.*, 1996, vol. 66, no. 6, p. 1042.
19. Aminova, R.M., Filatov, M.E., and Mironov, V.F., Abstracts of Papers, *XII Int. Conf. on Phosphorus Chemistry (ICPC)*, Jerusalem, 1995, p. 116.
20. Aminova, R.M., Mironov, V.F., and Filatov, M.E., *Proc. Fourth World Congress of Theoretically Oriented Chemists (WATOC'96)*, Jerusalem, 1996, p. 297.
21. Aminova, R.M., Filatov, M.E., Aganov, A.V., and Mironov V.F., *Materialy II Vserossiiskogo seminara "Novye dostizheniya YaMR v strukturnykh issledovaniyakh"* (Proc. II Russian Meeting "New Achievements of NMR in Structural Investigations"), Kazan, 1995, p. 77.
22. Aminova, R.M., Mironov, V.F., Filatov, M.E., and Burnaeva, L.M., Abstracts of Papers, *XI Int. Conf. on Phosphorus Chemistry*, Kazan, 1996, p. 193.
23. Mushkin, V.B., Mironov, V.F., Aminova, R.M., and Shamov, G.A., *Proc. Int. Symp. Comp. Assist. to Chem. Research (CACR-96)*, Moscow, 1996, p. 57.
24. Aminova, R.M., Shamov, G.A., Mushkin, V.B., Mironov, V.F., Konovalov, A.I., and Aganov, A.V., *Phosphorus, Sulfur, Silicon Relat. Elem.*, 1999, vol. 147, p. 265.
25. Savostina, L.I., Aminova, R.M., and Mironov, V.F., Abstracts of Papers, *Int. Conf. "Reaction Mechanisms and Organic Intermediates" (140 Years of Organic Structural Theory)*, St. Petersburg, 2001, p. 195.
26. Laikov, D.N., *Chem. Phys. Lett.*, 1997, vol. 281, p. 151.
27. Kirby, A., *The Anomeric Effect and Related Stereoelectronic Effects of Oxygen*, Heidelberg: Springer, 1983.
28. Nakamoto, M. and Akiba, K., *J. Am. Chem. Soc.*, 1999, vol. 121, no. 29, p. 6958.
29. Sase, S., Kano, N., and Kawashima, T., *J. Am. Chem. Soc.*, 2002, vol. 124, no. 33, p. 9706.
30. Schmidt, M.W., Baldridge, K.K., Boatz, J.A., Elbert, S.T., Gordon, M.S., Jensen, J.H., Koseki, S., Matsunaga, N., Nguyen, K.A., Su, S.J., Windus, T.L., Dupuis, M., and Montgomery, J.A., *J. Comput. Chem.*, 1993, vol. 14, no. 11, p. 1347.